The influence of chlorine on the dispersion of Cu particles on Cu/ZnO(0001) model catalysts

Ann W. Grant [a], Jeffrey T. Ranney [a], Charles T. Campbell [a,*], T. Evans [b] and G. Thornton [b]

[a] *Chemistry Department, University of Washington, Seattle, WA 98195-1700, USA*
[b] *Surface Science Research Centre and Chemistry Department, University of Manchester, Manchester M13 9PL, UK*

Received 10 December 1999; accepted 18 February 2000

One of the ways in which chlorine is thought to poison metal catalysts on oxide supports is by altering their dispersion. The effect of chlorine on Cu/ZnO(0001) model catalysts was studied by vapor-depositing Cu onto Zn-terminated ZnO(0001), both with and without preadsorbed Cl_2, using XPS, ion scattering spectroscopy (ISS), temperature-programmed desorption (TPD), work function, and band bending measurements. A disordered, but nearly close-packed overlayer of Cl adatoms forms at saturation with ~0.30 Cl adatoms per Zn site. Without Cl, vapor-deposited Cu grows in two-dimensional islands that cover ~33% of the ZnO, after which these islands thicken (i.e., as 3D Cu particles) while the clean ZnO between these Cu islands gets covered with Cu only very slowly. Preadsorbed Cl decreases the fraction of the surface that is covered by Cu islands by a factor of three, so Cl(a) either decreases the number of 2D Cu islands or their critical area before thickening. Both are consistent with weaker binding of Cu to the Cl-covered surface than to the clean ZnO. The TPD features for formate decomposition after HCOOH adsorption onto Cu/ZnO(0001) were suppressed with preadsorbed Cl, but the CO_2 : CO selectivity increased. When Cu was deposited onto Cl-presaturated ZnO, neither the Zn- nor Cu-formate peaks were observed, showing that Cl covers both the Zn sites and the growing Cu islands, as suggested by ISS also.

Keywords: Cu, ZnO, model catalysts, chlorine poisoning, chlorine adsorption, sintering, formate

1. Introduction

Many industrial catalysts consist of supported particles of an active transition metal dispersed across the surface of an oxide support. Chlorine is often present on the oxide surface in real catalyst preparations. It is thought that chlorine increases both the metal particle dispersion and resistance to thermal sintering although its presence has been shown to increase the metal crystallite size in other cases [1–8]. It is postulated that chlorine increases the mobility of metal oxide migration, so that it can accelerate both sintering and redispersion [7,8].

Most of the previous work on the effect of chlorine on metal particle dispersion has been performed on powdered catalysts. The most studied catalyst has been the hydrocarbon reforming catalyst, Pt/Al_2O_3, in which chlorine, either present on the support or in the gas phase, is thought to be necessary for the redispersion of the metal particles [9]. This is suggested to occur through the migration of PtO_xCl_y species under reaction conditions [7,9]. The low-temperature water–gas shift catalyst consists of Cu dispersed on ZnO/Al_2O_3, which is deactivated by the presence of chlorine. Even adsorption levels as low as 0.05% Cl, corresponding to 1–3 ppt chloride in the gas phase, can cause loss of activity. It was found also that the average particle size in the Cl-poisoned region of the reactor bed was 2.4 times the size of the Cu particles in the poison-free region [5,6]. In addition, recent work on Rh/CeO_2 catalysts showed that chlorine decreased the Rh dispersion when deposited from a $RhCl_3 \cdot H_2O$ solution as compared to a $Rh(NO_3)_3 \cdot H_2O$ solution [10].

Here, we address the effects of chlorine on the dispersion of Cu on ZnO by studying the effects of preadsorbed chlorine on the Cu particle morphology that evolves as Cu is vapor-deposited onto the Zn-terminated ZnO(0001) surface. A common industrial catalyst for the synthesis of methanol or higher alcohols, the water–gas shift reaction, and methanol steam reforming consists of Cu particles supported on ZnO/Al_2O_3 [11,12]. This work is part of an ongoing study of the growth and reactivity of ultrathin Cu particles on the polar faces of ZnO. Our studies [11,13,14] of the vapor deposition of Cu onto the Zn-terminated ZnO(0001) surface at room temperature and below found that Cu grows first as two-dimensional (2D) islands up to a certain critical coverage near 0.3 monolayers (ML). Above this coverage, these islands thicken into 3D islands but the clean ZnO spaces between the Cu particles fill only very slowly [11,13]. This occurs due to a kinetic limitation, since the islands thermodynamically prefer to be thicker and larger, as discussed thoroughly by Yoshihara et al. [14].

The reactions of formic acid with Cu particles on ZnO(0001) have also been studied previously [11]. Here, we use formic acid adsorption to probe the surfaces of the ZnO and the Cu particles produced by vapor deposition of Cu onto Cl-precovered ZnO(0001). Adsorbed formate, HCOO(a), can be easily produced on both Cu and ZnO surfaces by low exposures of formic acid in ultra-high vacuum (UHV) [15–21]. On Cu single crystals and

* To whom correspondence should be addressed.

Cu foil, not only does the formic acid desorb at ∼200–300 K, but also it partially decomposes to produce high coverages of adsorbed formate and H adatoms. The latter desorbs as H_2 at ∼350 K, and the Cu-bound formate decomposes at ∼480 K into $CO_2 + (1/2)H_2$ gas, probably via CO_2(a) and H(a) as transient adsorbed intermediates [19,20]. On ZnO(0001)–Zn, the formic acid molecularly desorbs mainly in temperature-programmed desorption (TPD) peaks at ∼200 and ∼365 K. It partially decomposes to produce high surface coverages of adsorbed formate and H adatoms, surface hydroxyls or bulk H in the ZnO. The Zn-bound formate decomposes at ∼575 K via two competing pathways:

dehydrogenation

$$\mathrm{HCOO(a)} \rightarrow \mathrm{CO_2(g)} + \mathrm{H(a)} \quad (1)$$

dehydration

$$\mathrm{HCOO(a)} \rightarrow \mathrm{CO(g)} + \mathrm{OH(a)} \quad (2)$$

The surface hydrogen product desorbs almost immediately as H_2(g). The hydroxyl products disproportionate almost immediately to give H_2O(g) and oxygen on or in the solid [15,16]. The adsorbed formate adopts a monodentate configuration, with a bond between one of its oxygen atoms and one Zn surface atom [16,22]. On Cu islands deposited on the oxygen-terminated ZnO(000$\bar{1}$)–O surface, it was found that the adsorbed formate is produced even on the thinnest Cu particles [23]. It adopts a bridging bidentate form on Cu terrace sites [24]. The TPD of formic acid from Cu particles on the Zn-terminated ZnO(0001)–Zn surface looks much like a superposition of features from Cu single crystals and ZnO(0001)–Zn, with some minor shifts in the Cu-bound formate decomposition peaks on the thinnest (i.e., 2D) Cu islands [11].

The purpose of the present experiment was to determine the effects of Cl(a) on the morphology and dispersion of Cu particles on ZnO(0001)–Zn. It was found that Cl(a) does decrease the dispersion of the Cu islands. We speculate that Cl increases the mobility of the Cu adatoms on the ZnO surface, enhancing its ability to approach more rapidly its thermodynamically-preferred state, large 3D islands on the surface [14]. A recent HREELS study of the growth of Cu on ZnO(0001)–O has shown that Cu initially nucleates at defect sites [24]. Perhaps Cl also passivates these nucleation sites, leading to a lower density of larger Cu islands.

2. Experimental

The experiments were performed in an ultrahigh vacuum (UHV) apparatus, described previously [11,25], with a base pressure of 10^{-10} Torr. It had capabilities for X-ray photoelectron spectroscopy (XPS), low-energy electron diffraction (LEED), low-energy ion scattering spectroscopy (ISS), and temperature-programmed desorption spectroscopy (TPD) using a line-of-sight quadrupole mass spectrometer interfaced to a computer for multiplexing masses.

All XPS spectra reported here used Al Kα radiation (1486.6 eV). The binding energy of the spectrometer was calibrated with the Zn($2p_{3/2}$) peak from the clean ZnO(0001) surface, which was set to 1021.7 eV [25]. All ISS spectra used 700 eV He^+ ion with scattering angle of 135°. All ISS spectra were taken with a primary ion energy of 700 eV, and a He pressure of 4×10^{-7} Torr as read by the ion gauge (the ion current is ∼20 nA/cm^2). The detection angle was normal to the surface in both XPS and ISS unless otherwise stated.

The temperature of the ZnO(0001) crystal could be varied between 140 and 1000 K with liquid-nitrogen cooling and resistive heating of a Mo support on which it was mounted. The TPD experiments were done with a heating rate of ∼5 K/s. Sample temperature was monitored with a thermocouple attached to the Mo support and calibrated as described elsewhere [11]. In preparing the ZnO(0001) sample, it was sputter-cleaned with 700 eV Ar^+ ions followed by annealing at 830–850 K to get a good p(1 × 1) LEED pattern as described in [13], where structural characterization of the clean, ordered surface is presented.

The formic acid used was 98% pure, with water as the main impurity, and was further purified with several freeze–pump–thaw cycles. The purity was verified with mass spectrometry. All formic acid exposures used a directed doser, as described previously [11].

Chlorine was dosed onto the sample from a mixture of Cl_2(g) + N_2(g) ($N_2 : Cl_2 = \sim 28:1$, or 3.5% Cl_2 in N_2) from a dosing tube connected to the gas reservoir by a leak valve. The dosing tube had a cosine-emitting orifice at the end, directly aimed at the sample, to give approximately a ten-fold higher dose than just filling the chamber with ambient gas. This enhancement factor of ten was used in reporting exposures, but should only be considered accurate to within a factor of two. Exposures are reported as Cl(2p) XPS intensities.

Copper was deposited with a home-made Cu doser. Details of this Cu doser are described elsewhere [13,23]. The Cu deposition rate was monitored by a quartz crystal thickness monitor, which was calibrated against the XPS Cu($2p_{3/2}$)/Zn($2p_{3/2}$) ratio for a 0.3 ML Cu dose as described in [13]. One Cu monolayer (ML) is defined as 1.77×10^{15} atoms/cm^2, the packing density of the Cu(111) surface plane, which is 2.1 Å thick. Thus, for 1.0 ML of Cu, there are 1.62 Cu atoms for each Zn surface atom or ZnO(0001) unit cell.

3. Results

3.1. Chlorine adsorption

As has been shown in [26], when the mixture of 3.5% Cl_2 in N_2 gas is dosed onto the Cl-free ZnO(0001) surface and saturates, it forms a disordered, but nearly close-packed

overlayer of Cl adatoms. This corresponds to a coverage of ∼0.30 Cl atoms per Zn surface atom or 3.45×10^{14} Cl atoms/cm^2, which is referred to here as 1.0 ML of Cl(a). The Cl(a) coverage is measured by the XPS intensity ratio (I_{Cl}/I^0_{Zn}), where I^0_{Zn} is the integrated intensity of the Cl-free Zn($2p_{3/2}$) peak, and I_{Cl} is the Cl(2p) peak area. The Cl(a) coverage is proportional to this ratio, which saturates at a value of 0.0048 at $\theta_{Cl} = 1.0$ ML [26]. The Zn ISS areas were found to decrease linearly with Cl(a) coverage to ∼0 at 1.0 ML, where only Cl(a) is seen in the ISS spectrum. Charge transfer from the surface to the adsorbate accompanied chlorine adsorption at 300 K onto ZnO(0001) [26], as predicted by Rodriguez in a theoretical study of the bonding of Cl to ZnO(0001) surfaces [27].

After annealing the ZnO(0001) surface to ∼750 K with ∼1.0 ML of Cl(a), there was a decrease of 35% in Cl(a) coverage as determined by the integrated intensity of the Cl(2p) XPS peak. However, no Cl-containing species (Cl, Cl_2, HCl, ZnCl, and CuCl) were seen desorbing with TPD. After adsorption of Cl_2 at 300 K on ZnO(0001), Hopkins and Taylor [28] found no discernable LEED pattern, but increased disorder. However, after annealing the surface to 700 K for 20 min, a $(2\sqrt{3} \times 2\sqrt{3})$ structure was seen along with a reduction in Cl coverage [28]. This implies ordering of the surface induced by annealing.

3.2. Cu film growth

3.2.1. Cu adsorption on Cl-free ZnO(0001)

Detailed studies of the structure, electronic properties, and growth kinetics of vapor-deposited Cu films have been reported previously [11,13] and are summarized here. Above ∼5% of a monolayer (ML), the Cu is practically charge neutral and clustered into islands with strong Cu–Cu bonding. Up to approximately a third of a ML, these islands are only one atom thick, and the Cu atoms do not sit in preferred substrate lattice sites. Thus, these are two-dimensional (2D) Cu islands. Above ∼33% of a ML, additional Cu adds predominantly on top of existing Cu islands, to make three-dimensional (3D) Cu islands that eventually adopt rotationally-aligned Cu(111) structure when the individual islands are 3 ML thick or thicker. After deposition of ∼1 ML of Cu, the Cu islands cover ∼40% of the surface and are ∼2.5 atomic layers thick on average [13]. Annealing above 500 K causes the islands to irreversibly thicken, thus uncovering part of the ZnO surface.

3.2.2. Cu co-adsorption with Cl on ZnO(0001)

The growth of Cu on ZnO(0001), as monitored by ISS, is affected by the presence of Cl(a), as illustrated in figure 1. The O ISS signal was followed, since the Cu and Zn signals cannot be resolved in ISS due to their similar masses. Below, we refer to the "Zn + Cu" ISS signal, in order to emphasize that the two signals cannot be resolved. As described in [13], the O ISS signal directly reflects the fraction of the ZnO surface that is not covered by Cu islands (or Cl). Figure 1 shows the changes in both the "Zn + Cu" and the O ISS signals with Cu coverage at two different Cl precoverages, as well as on the clean surface. The top curves in figure 1 show the attenuation of the O ISS and the increase in the "Zn + Cu" ISS signal with increasing Cu coverage on the Cl-free surface. These results are very similar to [11,13], summarized above. Notice that the O ISS curve attenuates by ∼45% at ∼1.8 ML of Cu. The middle curves show a much smaller attenuation of the O ISS signal with 0.53 ML of Cl(a) predosed to the surface. This amount of Cl(a) attenuates the O ISS intensity by ∼58%. Upon Cu deposition, the remaining O ISS intensity was attenuated by only 20% at ∼1.8 ML of Cu. The bottom set of curves show that the adsorption of ∼0.93 ML of Cl(a) almost completely attenuates the O ISS signal, so that it is difficult to monitor the further effects of increasing Cu coverage. Nevertheless, the percentage attenuation due to Cu appears again to be smaller than that on Cl-free ZnO.

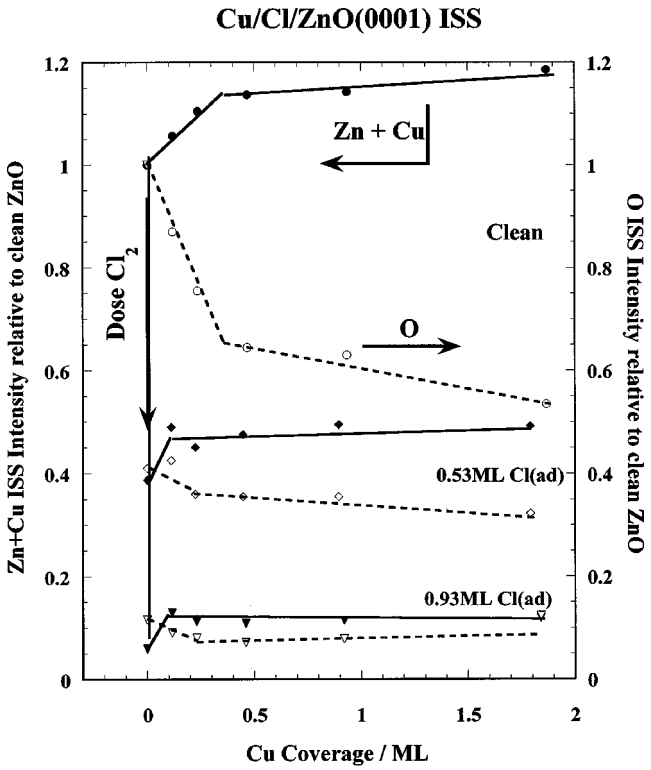

Figure 1. The change in the "Zn+Cu" and O ISS normalized intensities as a function of increasing Cu coverage on a Cl-free ZnO(0001) surface, on a surface predosed with 0.53 and 0.93 ML of Cl(a). Both the "Zn+Cu" (•) and O (○) ISS signals have been normalized to their respective clean surface values. The arrow on the left hand side is meant to guide the eye to increasing Cl_2 deposition.

Since in the presence of Cl(a) the fraction of the surface covered by Cu islands cannot be determined by the attenuation of the O ISS, the Cl ISS was examined. With both 0.53 and 0.93 ML of Cl preadsorbed on the surface, the Cl ISS was not significantly attenuated upon deposition of ∼0.5 ML of Cu, and only attenuated by ∼10%, on average, upon deposition of both ∼1 and ∼2 ML of Cu.

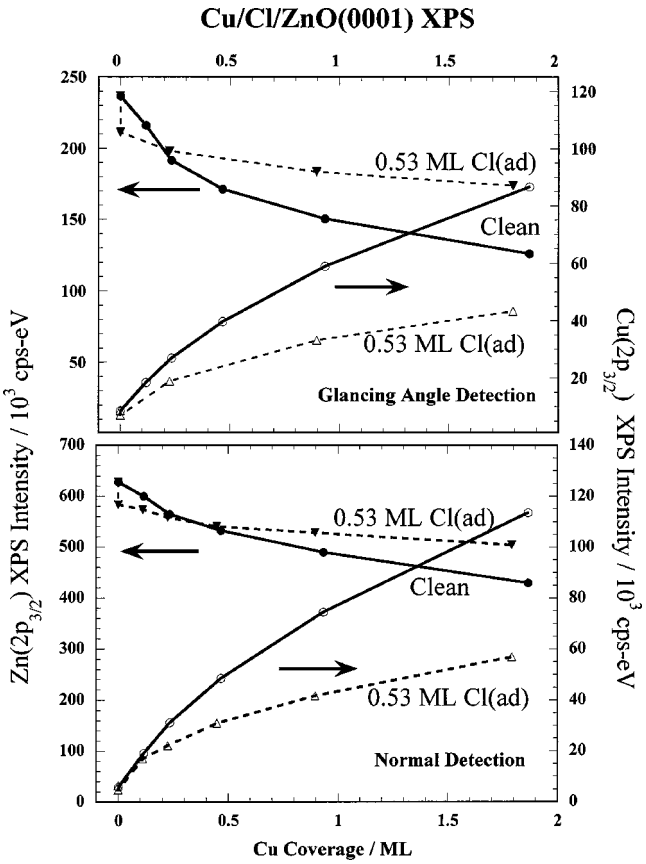

Figure 2. The variations in the $Zn(2p_{3/2})$ XPS integrated intensity and the $Cu(2p_{3/2})$ integrated intensity as a function of increasing Cu coverage, with and without a predosed 0.53 ML of Cl(a). The detection angle is 55° from normal in the top panel and normal in the bottom panel.

For 0.53 ML of Cl, the relative attenuation of the Cl ISS signal is only about half of the Cu-induced attenuation of the substrate O ISS signal.

The decrease in the Cu-induced attenuation of the O ISS signal with 0.53 ML of preadsorbed Cl could arise if the Cu islands cover much less of the surface when Cl(a) is present, or if the Cu islands grow underneath the Cl adatoms, so that they do not further attenuate the oxide substrate signal, or combinations of the above. The lack of comparable Cu-induced attenuation of the Cl ISS signal suggests that Cu moves underneath the Cl, at least to some extent.

In order to determine the fraction of the surface covered by Cu islands in the presence of Cl(a), XPS intensities were examined. In figure 2, the changes in both the $Cu(2p_{3/2})$ and $Zn(2p_{3/2})$ XPS intensities with increasing Cu coverage on both a Cl-free surface and on a surface with 0.53 ML of Cl(a) are presented at both normal angle (bottom panel) and at 55° from normal detection (top panel). At both normal and 55° from normal detection, the rise in the $Cu(2p_{3/2})$ XPS intensity on the Cl-covered surface is much smaller than on the Cl-free surface. In addition, the attenuation of the $Zn(2p_{3/2})$ XPS intensity was not as great as on the Cl-free surface. This clearly indicates that the Cu islands are thicker and cover fractionally less of the surface when Cl(a) is preadsorbed.

The fraction of the surface, f, covered by Cu islands when Cl(a) is present can be estimated from the measured XPS intensities of both the $Cu(2p_{3/2})$ and $Zn(2p_{3/2})$ peaks by comparing the intensities with and without Cl(a) at the same Cu dose. Assuming that all Cu-covered patches have the same thickness, t, given by $t = t_{\mathrm{Cu}}^{\mathrm{QCM}}/f$, where $t_{\mathrm{Cu}}^{\mathrm{QCM}}$ is the average thickness of deposited Cu known from the quartz crystal microbalance measurement (assuming unit sticking probability for Cu), then the measured XPS intensity ratios are given by

$$\frac{I_{\mathrm{Cu}}\mathrm{w/Cl}}{I_{\mathrm{Cu}}\mathrm{w/o}} = \frac{f\left(1-\exp\left(-\frac{t_{\mathrm{Cu}}^{\mathrm{QCM}}/f}{\lambda_{\mathrm{Cu}}\cos\theta_{\mathrm{d}}}\right)\right)\exp\left(-\frac{t_{\mathrm{Cl}}}{\lambda_{\mathrm{Cu}}\cos\theta_{\mathrm{d}}}\right)}{f^{0}\left(1-\exp\left(-\frac{t_{\mathrm{Cu}}^{\mathrm{QCM}}/f^{0}}{\lambda_{\mathrm{Cu}}\cos\theta_{\mathrm{d}}}\right)\right)} \quad (3)$$

and

$$\frac{I_{\mathrm{Zn}}\mathrm{w/Cl}}{I_{\mathrm{Zn}}\mathrm{w/o}} = \frac{\left\{1-f+f\left(1-\exp\left(-\frac{t_{\mathrm{Cu}}^{\mathrm{QCM}}/f}{\lambda_{\mathrm{Zn}}\cos\theta_{\mathrm{d}}}\right)\right)\right\}\exp\left(-\frac{t_{\mathrm{Cl}}}{\lambda_{\mathrm{Zn}}\cos\theta_{\mathrm{d}}}\right)}{1-f^{0}+f^{0}\left(1-\exp\left(-\frac{t_{\mathrm{Cu}}^{\mathrm{QCM}}/f^{0}}{\lambda_{\mathrm{Zn}}\cos\theta_{\mathrm{d}}}\right)\right)}. \quad (4)$$

Here, f^0 is the fraction of the Cl-free surface covered by Cu islands measured by O ISS, as described in [11], I_x is the XPS intensity of peak x, either with Cl(a) present (w/Cl) or without Cl (w/o), λ_{Cu} is the inelastic mean free path of $Cu(2p_{3/2})$ photoelectrons in Cu(s), λ_{Zn} is the inelastic mean free path of $Zn(2p_{3/2})$ photoelectrons in ZnO(s), θ_{d} is the detection angle, and t_{Cl} is the average thickness of the Cl adlayer. Here, t_{Cl} was experimentally determined from both the attenuation of the $Zn(2p_{3/2})$ XPS peak and the ratio of the Cl(2p) to the clean $Zn(2p_{3/2})$ ratio, as described in [26]. At 1 ML of Cl(a), t_{Cl} was 1.3 Å. The values of λ_{Cu} (12 Å) and λ_{Zn} (8 Å) were determined on this same system previously [13]. Using the data in figure 2 for a Cl coverage of 0.53 ML, the fraction of the surface covered by Cu islands, f, was determined at both detection angles using both equations (3) and (4), and these four values were averaged at each Cu coverage (using double weighting for the more surface-sensitive data at $\theta_{\mathrm{d}} = 55°$). These results for 0.53 ML Cl are shown in figure 3. As can be seen, this predosed Cl reduces the fraction of the surface covered by Cu islands to $\sim 1/3$ of its value for Cl-free ZnO(0001) at all Cu coverages studied.

Similar XPS data to figure 2 were collected at a variety of Cl precoverages and Cu coverages, and analyzed in the same way. The results are summarized in figure 3. Notice that when a large amount of Cl is present on the surface, it has a large effect on the fraction of the surface covered by Cu islands. When only 0.05 ML of Cl is present, there is a similarly large initial effect on the fraction of the surface covered by Cu islands, but the effect becomes much less pronounced when the Cu coverage greatly exceeds the Cl coverage. This indicates that the effect of one Cl adatom can only extend to a limited number of postdosed Cu atoms.

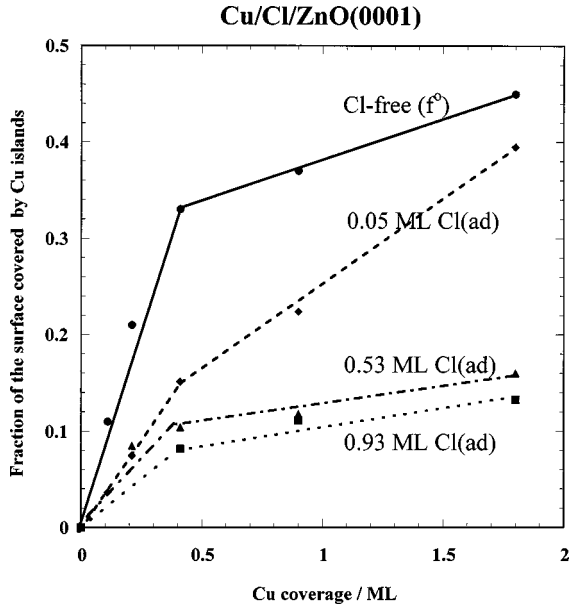

Figure 3. Variations with Cu coverage in the fraction of the surface covered by Cu islands (as determined by quantitative XPS analysis) for different amounts of predosed Cl(a). The top curve for Cl-free ZnO(0001)–Zn was determined by O ISS and gives the value of f^0 used in equations (3) and (4) to calculate the fractions with Cl(a) present.

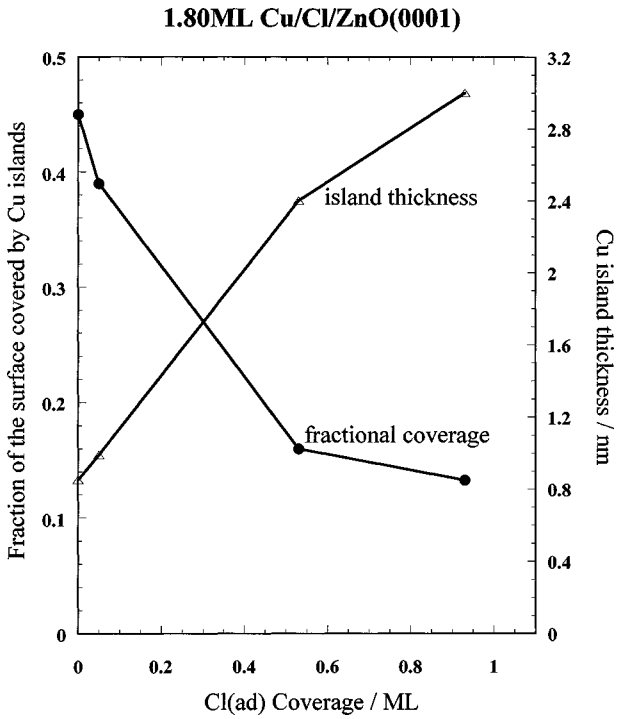

Figure 4. Variations with Cl precoverage in the fraction of the ZnO(0001) surface covered by Cu islands and the Cu island thickness (as determined by XPS) for 1.8 ML of deposited Cu. There is an approximately three-fold decrease in the fractional coverage of Cu islands as θ_{Cl} increases.

Figure 4 shows the data of figure 3 at 1.8 ML of Cu, replotted to show directly the effect of Cl coverage on f and the island thickness. There is an almost three-fold decrease in the fraction of the surface which is covered by Cu islands as Cl is added. Even 5% of a ML of Cl(a) leads to a ∼15% decrease in the fraction of the surface covered by Cu islands, as shown. This effect is even more dramatic at lower Cu coverages (see figure 5). The Cl-induced decrease in f is accompanied by a corresponding increase in the Cu island thickness.

In the absence of Cu, the Zn($2p_{3/2}$) binding energy (BE) is shifted by ∼0.8 eV upon Cl_2 saturation, due to a Cl-induced band bending associated with electron transfer from the ZnO depletion zone to Cl(a) [26]. However, upon Cu deposition to the Cl-saturated surface, the Zn($2p_{3/2}$) BE is shifted back to the clean ZnO(0001) value, suggesting that somehow the Cu relaxes this charge transfer.

The Cu($2p_{3/2}$) peak shifted slightly to lower binding energy with increasing Cu coverage from 0.1 ML, eventually reaching ∼932.3 eV at 1–2 ML coverage, whether the Cu was deposited onto clean or Cl-predosed ZnO(0001). (The final value is within the range of values reported for bulk Cu of 932.2–932.6 eV [25].) For Cl-free ZnO, this shift was ∼0.5 eV, similar to the value of 0.4 eV seen on the O-terminated face of ZnO [25]. This was attributed to final-state effects associated with the increasing size of Cu particles composed of essentially neutral Cu atoms, and we propose the same explanation here. As noted earlier [25], the Cu($2p_{3/2}$) peak energy is about the same for Cu^+ as for Cu^0, so we cannot rule out contributions from Cu^+. However, since no characteristic satellites from Cu^{2+} were seen [29] even with predosed Cl, we can rule out Cu^{2+}.

To test whether the order of dosing of Cl and Cu has any effect on the Cu morphology, an experiment with the reverse dosing order was done. That is, 0.8 ML of Cu was first dosed to the surface, and a saturation coverage of Cl was added. The fraction of the surface covered by Cu islands was calculated as above based on the XPS intensities. Before adding Cl, the Cu islands covered ∼37% of the surface, as observed by O ISS. After the Cl(a) was added, XPS showed that the Cu islands covered only ∼20% of the surface. In contrast, when the reverse dosing sequence was used (i.e., Cl first), only 11% of the surface was covered by Cu islands (see above). Thus, Cu clusters into thicker islands when Cl is dosed first.

To test the effects of Cl(a) on the sintering rate of the Cu particles, two differently prepared ZnO(0001) surfaces, both with ∼0.8 ML of Cu predeposited at 300 K, were heated to ∼800 K at a rate of ∼5 K/s, immediately cooled, and examined by XPS. The first surface was Cl-free and at 300 K had Cu islands covering ∼37% of the surface. The second surface was Cl-saturated after the Cu deposition leaving ∼20% of the surface covered by Cu islands at 300 K. Annealing to ∼800 K left ∼10% of the surface covered by Cu islands on the Cl-free surface, whereas on the Cl-saturated surface only ∼5% of the surface was covered by Cu islands after annealing. This indicates that Cl(a) facilitates the sintering of Cu.

After annealing the above Cl-saturated Cu particles, a strong satellite peak appeared at ∼10 eV lower kinetic

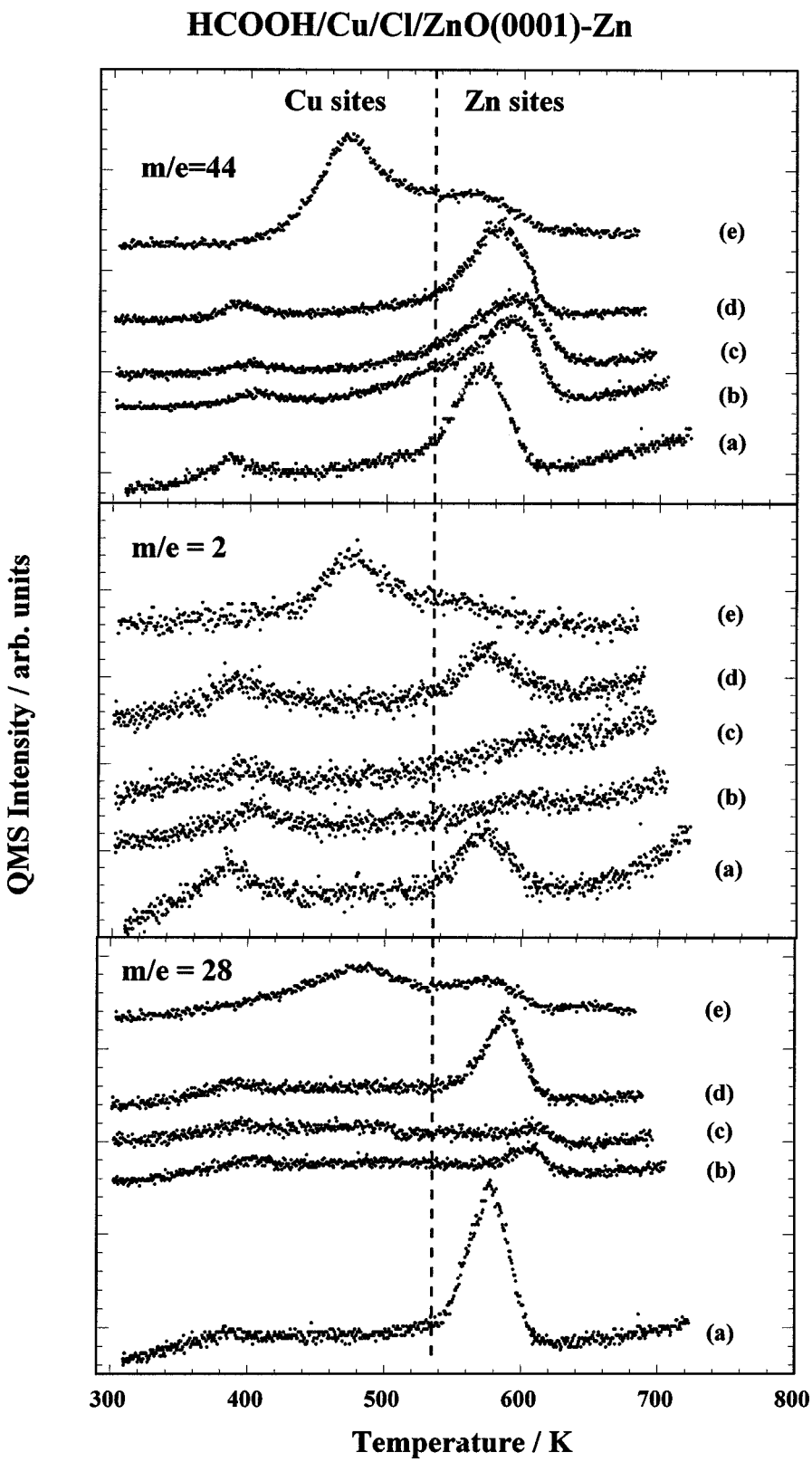

Figure 5. The effect of Cl(a) on the TPD spectra recorded after a saturation dose of HCOOH (∼3 L, taking the enhancement factor of the doser into account) onto ZnO(0001)–Zn at 300 K with different pretreatments. The two panels show the representative products of formate decomposition via dehydration and dehydrogenation: CO ($m/e = 28$), CO_2 ($m/e = 44$), and H_2 ($m/e = 2$), respectively (see text). (a) Clean ZnO(0001), (b) 0.6 ML of Cl(a) predeposited on ZnO(0001), (c) 0.6 ML of Cl(a) followed by 0.9 ML of Cu on ZnO(0001)–Zn, (d) same surface as (c) but after annealing the surface to ∼700 K before dosing the HCOOH, and (e) 1.8 ML Cu predosed on ZnO(0001). Baselines have been offset for clarity.

energy than the main Cu(2p) XPS. This peak is characteristic of Cu^{2+} [29]. Its intensity indicated that ∼25% of the Cu was converted to Cu^{2+}, probably in the form of $CuCl_2$(solid). It is conceivable that CuCl(s) is forming also, but we have no spectroscopic evidence since the Cu and Cu(I) binding energies are identical in XPS, and the Zn AES lines obscure the small Cu AES signal. Low-index Cu single-crystal surfaces form Cl(a) and then CuCl(s) islands upon further Cl_2 exposure [30–32]. Consider the standard enthalpy changes for the following two reactions at 298 K [33]:

$$ZnCl_2(s) \rightarrow Zn(s) + Cl_2(g) \quad (\Delta H^0 = 99.20 \text{ kcal/mol})$$

and

$$Cu(s) + Cl_2(g) \rightarrow CuCl_2(s) \quad (\Delta H^0 = -52.60 \text{ kcal/mol})$$

One can see that the net reaction

$$ZnCl_2(s) + Cu(s) \rightarrow Zn(s) + CuCl_2(s)$$
$$(\Delta H = 46.6 \text{ kcal/mol})$$

is enthalpically unfavorable. The reaction leading to the formation of CuCl(s) is also entropically unfavorable with a $\Delta H = 33.60$ kcal/mol [33]. Thus, Zn(s) likes Cl better than Cu(s). However, Cu(s) could easily like Cl better than ZnO(s), since the oxygen atoms present already satisfy Zn's desire for anionic neighbors. Churturvedi et al. similarly showed that the adsorption of S_2 on Cu-deposited ZnO leads to the formation of copper sulfides, especially at >0.5 ML of S_2 [34]. In addition, Yoshihara et al. found evidence that formate does not strongly modify the Cu particle morphology, since the attenuation of the Zn-formate TPD peaks (∼55%) was reasonably consistent with the loss of Zn sites due to vapor-deposited Cu as determined by ISS [11].

3.3. HCOOH adsorption

3.3.1. HCOOH adsorption on Cl-free Cu/ZnO(0001)

In order to address the question of whether or not Cl(a) is present on the Cu islands, a new probe was introduced: formic acid (HCOOH) chemisorption and TPD. As discussed in section 1, adsorbed formic acid on ZnO(0001) decomposes to produce adsorbed formate, via a mechanism like [15,16]

$$HCOOH(a) \rightarrow HCOO(a) + H(a)$$

Peaks for CO, H_2O, CO_2, and H_2 are observed nearly simultaneously at ∼575 K in TPD, due to adsorbed formate decomposing via the two competing paths [15,16]:

dehydrogenation

$$HCOO(a) \rightarrow CO_2(g) + H(a) \quad (1)$$

dehydration

$$HCOO(a) \rightarrow CO(g) + OH(a) \quad (2)$$

The H(a) desorbs as H_2(g) and the OH(a) as H_2O(g). Figure 5 shows CO ($m/e = 28$), CO_2 ($m/e = 44$), and H_2 ($m/e = 2$) evolution in the TPD spectra from the clean ZnO(0001) surface and from Cu films deposited on ZnO(0001), after dosing ∼3.0 L (1 langmuir = 1 L = 10^{-6} Torr s, taking into consideration the enhancement factor (∼10) of the doser) of formic acid at 300 K. This formic acid dose has been shown by Yoshihara et al. [11] to sufficiently saturate the formate decomposition peaks at ∼575 K. The small peak at ∼380–400 K seen in all three masses can be attributed to molecular desorption of chemisorbed formic acid [11,15]. It is consistent with its cracking pattern measured directly in this instrument at a comparable partial pressure. As expected based on the dehydration mechanism above, the TPD peaks for H_2O ($m/e = 18$, not shown) are very similar to the curves for CO ($m/e = 28$) after correction for the CO_2 cracking pattern, although $m/e = 18$ is somewhat noisier due to higher relative background partial pressure of water. Curves (a) and (e) for clean ZnO(0001) and Cl-free ZnO(0001) with 1.8 ML of Cu, respectively, are essentially identical to those presented by Yoshihara et al. [11].

In curves (e) of figure 5, the Cu should be predominantly in the form of three-dimensional islands that are ∼4 atomic layers thick covering ∼45% of the surface at this coverage [13]. The sharp new peak seen in both the $m/e = 2$ and 44 curves at 480 K can be attributed to formate decomposition into $CO_2 + H_2$ on Cu sites, since the TPD temperature is very close to that from formate decomposition after dosing formic acid to bulk metallic Cu surfaces (∼475–480 K) ([19–21], and references therein). A weak new peak also appeared at this temperature for $m/e = 28$, which is mainly attributable to the cracking pattern of the CO_2 product (for which the 28/44 ratio is ∼1/6 [11]). Clearly, the TPD of formic acid from Cu particles on ZnO(0001) looks very much like a superposition of features from Cu single crystals and ZnO(0001), indicating the presence of both Cu and Zn sites for formate decomposition. In addition, Yoshihara et al. found evidence that formate does not strongly modify the Cu particle morphology, since the attenuation of the Zn-formate TPD peaks (∼55%) was reasonably consistent with the loss of Zn sites due to vapor-deposited Cu as determined by ISS [11].

3.3.2. HCOOH adsorption on Cu films grown on Cl-predosed ZnO(0001)

Figure 5 also shows the TPD spectra of formate decomposition from the Cl-predosed ZnO(0001) surface (b), and from a Cu film deposited on the Cl-predosed ZnO(0001) surface (c), all with the same ∼3 L exposure of formic acid at 300 K. On the surface precovered with 0.6 ML of Cl(a), curves (b), the CO peak seen at ∼575 K on the Cl-free surface is shifted upward to ∼605 K and is attenuated by ∼80%. The water peak (not shown) is attenuated by ∼25%. The CO_2 peak is broadened and the peak maximum is shifted up in temperature by ∼20 K. The H_2 peak, however, is attenuated by ∼70%. This severe attenuation of the CO peak, without a subsequent attenuation of the

CO_2 peak, indicates that the branching ratio between dehydrogenation and dehydration, reactions (1) and (2) above, is altered by the presence of Cl(a), such that dehydrogenation is strongly favored. Note that the fate of the H(a) produced by this reaction also seems to have been altered by the presence of the Cl(a). It now appears as H_2O instead of as H_2. Perhaps this is because Cl(a), by bonding to the Zn cations, makes it easier for this hydrogen to abstract lattice oxygen and partially reduce the ZnO surface. The effects of Cl(a) on the TPD of formate are discussed in more detail in [26].

In curves (c) of figure 5, 0.9 ML of Cu was dosed to the ZnO, after the addition of 0.6 ML of Cl(a), but before the HCOOH. This produces Cu islands which cover ∼14% of the surface, and are ∼6.5 atomic layers thick (see above). The presence of Cl(a) in curves (c) decreases the amount of adsorbed Zn formate and changes the selectivity of its decomposition towards more dehydrogenation, just as in curves (b). In addition, there are no peaks at the temperature of ∼480 K, characteristic of formate decomposition on Cu-formate sites as there were in curves (e). Curves (c) look almost identical to curves (b), which are from a surface with the same Cl coverage but no Cu. However, XPS shows that surface (c) has Cu islands which cover ∼33% the area of the Cu islands in curves (e). Thus, with all other things being equal, peaks for CO_2 and H_2 should be seen at ∼480 K in curves (c) with $\sim 1/3$ the intensity of those in curves (e). Clearly, if CO_2 and H_2 peaks are present there, they are in much lower intensity. This we attribute to Cl(a) covering the surface of the Cu islands, even though the Cu was dosed *after* the Cl. This is consistent with the ISS results discussed in section 3.2.2, which showed very little growth in the "Zn + Cu" ISS signals and little loss in the Cl ISS signal upon increasing Cu coverage when Cl(a) had been predosed to the surface. Apparently Cl(a) moves up on top of the Cu islands as they grow during Cu vapor deposition, and thus poison the Cu sites with respect to formate production from HCOOH dosing. Thus, the deposited Cu seems to displace the underlying Cl.

After annealing the surface in curves (c) to ∼700 K, the HCOOH TPD spectra in curves (d) resulted. Above 500 K, Cu islands start to thicken into 3D islands, uncovering slightly more of the ZnO substrate, at least when Cl(a) is not present [11]. Curves (d) with 0.60 ML of Cl(a) and 0.9 ML of Cu present show a marked increase in the amount of formate decomposing from Zn sites after annealing. The CO_2 peak area remained about the same after annealing surface (c), but the CO peak area increased by approximately five-fold. This indicates that the dehydration pathway is once again available for formate decomposition at Zn sites, which are once again available to adsorb surface hydroxyls. In this case, on the Cl- and Cu-predosed surface, annealing restored the formate TPD areas to ∼65% of their clean surface total. Since the Cu islands only cover ∼14% of the surface even before annealing, the huge increase in formate decomposition intensity from Zn sites after annealing *cannot* simply be attributed again to the uncovering of Zn sites as Cu further agglomerates. Instead, this must arise because Cl adatoms are leaving the Zn sites and moving onto or into the Cu particles upon annealing, or simply moving into the bulk of the ZnO. When an even higher Cl coverage on Cu-free ZnO was annealed to an even higher temperature, only ∼35% of the Cl was lost from the surface (see above). The more dramatic loss of Cl seen here via the formate TPD must somehow be associated with the presence of Cu, probably related to a transfer of Cl(a) from Zn sites to the Cu.

Supporting this explanation, there is no evidence of formate decomposition at the Cu sites at ∼480 K indicating that Cl(a) is still covering the Cu islands after the anneal. Indeed, after the Cu islands had been annealed with Cl(a) on the surface, they were partially converted to $CuCl_2$ (see above).

4. Discussion

Some of the same conclusions about the effect Cl(a) has on the fraction of the surface covered by Cu islands drawn from the XPS data (figures 2, 4, and 5) can be drawn from the ISS data also (figure 1). Assuming that the "Zn + Cu" ISS signal is an area-weighted linear combination of the relative intensity of the Cu signal from the Cu islands, J_{Cu}, and the relative intensity of the Zn signal from Cu-free areas, J_{Zn}, then the intensity of the "Zn + Cu" ISS signal should be

$$J_{Zn+Cu} = f J_{Cu} + (1 - f) J_{Zn}. \tag{5}$$

When 1.8 ML of Cu was deposited on a Cl-free ZnO(0001) surface, the fraction of the surface covered by Cu islands, as measured by O ISS, was $f = 0.45$, and the measured intensity of the "Zn + Cu" signal, J_{Zn+Cu}, was 1.19, after being normalized to the Zn peak area from clean ZnO (0001): $J_{Zn} = 1.0$. From equation (5), we can calculate that the relative intensity of Cu from clean Cu islands, J_{Cu}, is 1.42. If we assume (incorrectly) that Cl(a) does not cover the Cu islands upon Cu deposition to a Cl-precovered surface, then J_{Cu} should be independent of the Cl precoverage and the same as the Cl-free value of 1.42. For a given Cl precoverage, J_{Zn} is directly measured by the "Zn + Cu" ISS signal after Cl dosing (but before Cu), normalized to that of clean ZnO ($J_{Zn} = 1.0$). One can estimate f for a given Cu coverage on Cl-predosed ZnO(0001) from equation (5) using this value and the measured value of J_{Zn+Cu}. For example, for a Cl precoverage of 0.53 ML, J_{Zn} is 0.39 and J_{Zn+Cu} is 0.49 at 1.8 ML of Cu (see figure 1), giving $f = 0.10$. This is less than the value of $f = 0.16$ calculated from XPS intensities, because Cl(a) partially covers the Cu islands too. Similarly, for 0.93 ML Cl(a) and 1.8 ML of Cu, this method gives $f = 0.044$, which is a much smaller value than that calculated from XPS intensities ($f = 0.13$). Again, this clearly shows that Cl(a) partially covers the Cu islands.

Why does the presence of Cl(a) lead to thicker Cu particles? There are several reasons. The first is a simple

site blocking argument. Cu requires defect sites in order to nucleate islands on the surface during vapor deposition onto ZnO [14]. The presence of Cl(a) could effectively poison the available defect sites, decreasing the availability of nucleation sites for the Cu islands to form, lowering their number density. This, therefore, increases the Cu island thickness for the same amount of deposited Cu [14]. There was no evidence however in XPS for the presence of ClO_x moieties [26]. Another explanation is that there is an enhanced mobility of Cu, perhaps as Cu–Cl moieties, such that the diffusion constant of Cu increases with the presence of Cl. Since the number density of metal islands is proportional to $(F/D_0)^{1/3}$ (in the case of homogeneous nucleation), where F is the metal vapor flux and D_0 is the diffusion coefficient of an isolated Cu adatom across the oxide surface [14], if the rate constant for diffusion increases, the number density of islands decreases. Thus, if Cl(a) doubles the rate constant for diffusion or mobility of Cu islands, the number density of Cu islands will be decreased by 20%. Bartholomew et al. proposed an increased mobility of the metal adatoms in the presence of Cl(a) [7,8]. Recently, beautiful STM images have revealed how adsorbed H atoms bond directly to Pt atoms or Pt(110) and accelerate their diffusion [35].

In addition, there is some evidence that both S and Cl enhance the mobility of other noble metals (mainly Au, in electrochemical cells) [36]. This was attributed to the large strength of their bonding to the metal, which weakens the metal–metal bond strength. This lowers the diffusion barrier and thus the metal atoms should show a higher mobility, as suggested above. If Cl enhances the mobility of Cu adatoms moving around on 2D Cu islands, this would increase the so-called critical island area that is reached before the Cu island thickens [14]. This would also decrease f, as observed. Enhanced Cu mobility should increase the rate of particle sintering and catalyst redispersion as well. Enhanced mobility is a typical result of weaker adsorption strength, which suggests that Cu adsorbs more weakly to Cl-precovered ZnO.

Our results are consistent with the effect of chlorine in industrial Cu catalysts for the low-temperature water–gas shift reaction. In ammonia plants that utilize the water–gas shift reaction, there is a distribution of chlorine across the catalyst bed. The Cu crystallite size is about 140 Å in the Cl-free part of the bed, whereas the average Cu crystallite size is about 330 Å in the Cl-containing part of the bed. This ratio of the Cl-containing to Cl-free crystallite size is $\sim$2.4, consistent with our data which showed an increase in the particle size in the presence of Cl of approximately three-fold [5,6].

5. Conclusions

The preadsorption of Cl(a) on the surface of ZnO(0001)–Zn alters the growth morphology of Cu particles under Cu metal vapor deposition. The Cu islands grow thicker and cover much less of the surface than on Cl-free ZnO(0001) surfaces. This decreases the dispersion of these Cu/ZnO model catalysts, by decreasing the Cu particle's total surface area. Using formic acid TPD and ISS, we have shown that the Cl(a) covers the Cu islands as well as the ZnO substrate. The Cl(a) is held more strongly to the Cu sites than the Zn^{2+} sites. The presence of Cl(a) alters the formate decomposition branching ratio towards more CO_2 than CO product.

Acknowledgement

Financial support for this research by the Department of Energy, Office of Basic Energy Sciences, Division of Chemical Sciences, and a NATO collaborative grant is gratefully acknowledged. The authors would like also to thank Jim Gladden for technical support.

References

[1] J.P. Bournonville and G. Martino, in: *Catalyst Deactivation*, eds. B. Delmon and G. Froment (Elsevier, Amsterdam, 1980) p. 159.
[2] H. Lieske, G. Lietz, H. Spindler and J. Völter, J. Catal. 81 (1983) 8.
[3] G. Lietz, H. Lieske, H. Spindler, W. Hanke and J. Völter, J. Catal. 81 (1983) 17.
[4] G.I. Straguzzi, H.R. Aduriz and C.E. Gigola, J. Catal. 66 (1980) 171.
[5] P.J. Denny and M.V. Twigg, in: *Catalyst Deactivation*, eds. B. Delmon and G. Froment (Elsevier, Amsterdam, 1980) p. 585.
[6] P.N. Hawker, Hydrocarbon Process. (April 1982).
[7] C.H. Bartholomew, in: *Catalyst Deactivation*, eds. C.H. Bartholomew and G.A. Fuentes (Elsevier, Amsterdam, 1997) p. 585.
[8] C.H. Bartholomew, in: *Catalyst Deactivation*, Stud. Surf. Sci. Catal., Vol. 88, eds. B. Delmon and G.F. Froment (Elsevier, Amsterdam, 1994).
[9] J.B. Butt and E.E. Petersen, *Activation and Deactivation and Poisoning of Catalysts* (Academic Press, San Diego, 1988).
[10] D.I. Kondarides and X.E. Verykios, J. Catal. 174 (1998) 52.
[11] J. Yoshihara and C.T. Campbell, Surf. Sci. 407 (1998) 256.
[12] N. Takezawa and N. Iwasa, Catal. Today 36 (1997) 45.
[13] J. Yoshihara, J.M. Campbell and C.T. Campbell, Surf. Sci. 406 (1998) 235.
[14] J. Yoshihara, S.C. Parker and C.T. Campbell, Surf. Sci. 439 (1999) 153.
[15] J.M. Vohs and M.A. Barteau, Surf. Sci. 176 (1986) 91.
[16] W.T. Petrie and J.M. Vohs, Surf. Sci. 245 (1991) 315.
[17] S. Akhter, K. Lui and H.H. Kung, J. Phys. Chem. 89 (1985) 1958.
[18] S. Akhter, W.H. Cheng, K. Lui and H.H. Kung, J. Catal. 85 (1984) 437.
[19] F.C. Henn, J.A. Rodriguez and C.T. Campbell, Surf. Sci. 236 (1990) 282.
[20] J. Yoshihara and C.T. Campbell, J. Catal. 161 (1996) 776.
[21] A. Ludviksson, R. Zhang, C.T. Campbell and K. Griffiths, Surf. Sci. 313 (1994) 64.
[22] W.T. Petrie and J.M. Vohs, Surf. Sci. 274 (1992) L503.
[23] C.T. Campbell, Crit. Rev. Surf. Chem. 4 (1994) 49.
[24] G. Thornton, S. Crook and Z. Chang, Surf. Sci. 415 (1998) 122.
[25] K.H. Ernst, A. Ludvikssson, R. Zhang and J. Yoshihara, Phys. Rev. B 47 (1993) 13782.
[26] A.W. Grant, A. Jameison and C.T. Campbell, Surf. Sci., submitted.
[27] J.A. Rodriguez, Surf. Sci. 222 (1989) 383.
[28] B.J. Hopkins and P.A. Taylor, J. Phys. C 9 (1976) 571.
[29] J. Ghijsen, L.H. Tjeng, J. van Elp, J. Eskes, J. Erdyrtink, G.A. Sawatzky and M.T. Czyzyk, Phys. Rev. B 38 (1988) 11322.

[30] C.Y. Nakakura, G. Zheng and E.I. Altman, Surf. Sci. 401 (1998) 173.
[31] K.N. El'tov, G.Ya. Zueva, A.N. Klimov, V.V. Martynov and A.M. Prokhorow, Surf. Sci. 251/252 (1991) 753.
[32] M. Galeotti, B. Cortigiani, U. Bardi, B.V. Andrysushechkin, A.N. Klimov and K.N. El'tov, J. Electron Spectrosc. Relat. Phenom. 76 (1995) 91.
[33] D.R. Lide, ed., *CRC Handbook of Chemistry and Physics*, 71st Ed. (The Chemical Rubber Company, Boca Raton, 1990).
[34] S. Churturvedi, J.A. Rodriguez and J. Hrbek, J. Phys. Chem. B 101 (1997) 10860.
[35] S. Horch, H.T. Lorensen, S. Helveg, E. Lægsgaard, I. Stensgaard, K.W. Jacobsen, J.K. Nørskov and F. Besenbacher, Nature 398 (1999) 134.
[36] S.J. Stanick, A.N. Parikj, D.L. Allara and P.S. Weiss, J. Phys. Chem. 98 (1994) 11136.